POTSDAM-INSTITUT FÜR
KLIMAFOLGENFORSCHUNG

AGU PUBLICATIONS

JGR

Journal of Geophysical Research: Biogeosciences

RESEARCH ARTICLE
10.1002/2015JG003036

Key Points:
- Three important drivers of burned area for Europe were analyzed
- Fire-vegetation interaction emerged as an important uncertainty
- Eastern Europe was simulated as an emerging new fire-prone region

Supporting Information:
- Supporting Information S1

Correspondence to:
M. Wu,
minchao.wu@nateko.lu.se

Citation:
Wu, M., W. Knorr, K. Thonicke, G. Schurgers, A. Camia, and A. Arneth (2015), Sensitivity of burned area in Europe to climate change, atmospheric CO_2 levels, and demography: A comparison of two fire-vegetation models, *J. Geophys. Res. Biogeosci.*, *120*, 2256–2272, doi:10.1002/2015JG003036.

Received 30 APR 2015
Accepted 14 OCT 2015
Accepted article online 20 OCT 2015
Published online 14 NOV 2015

Sensitivity of burned area in Europe to climate change, atmospheric CO_2 levels, and demography: A comparison of two fire-vegetation models

Minchao Wu[1], Wolfgang Knorr[1], Kirsten Thonicke[2], Guy Schurgers[3], Andrea Camia[4], and Almut Arneth[5]

[1]Department of Physical Geography and Ecosystem Science, Lund University, Lund, Sweden, [2]Potsdam Institute for Climate Impact Research, Potsdam, Germany, [3]Department of Geosciences and Natural Resource Management, University of Copenhagen, Copenhagen, Denmark, [4]Institute for Environment and Sustainability, European Commission, Joint Research Centre, Ispra, Italy, [5]Institute of Meteorology and Climate Research - Atmospheric Environmental Research, Karlsruhe Institute of Technology, Garmisch-Partenkirchen, Germany

Abstract Global environmental changes and human activity influence wildland fires worldwide, but the relative importance of the individual factors varies regionally and their interplay can be difficult to disentangle. Here we evaluate projected future changes in burned area at the European and sub-European scale, and we investigate uncertainties in the relative importance of the determining factors. We simulated future burned area with LPJ-GUESS-SIMFIRE, a patch-dynamic global vegetation model with a semiempirical fire model, and LPJmL-SPITFIRE, a dynamic global vegetation model with a process-based fire model. Applying a range of future projections that combine different scenarios for climate changes, enhanced CO_2 concentrations, and population growth, we investigated the individual and combined effects of these drivers on the total area and regions affected by fire in the 21st century. The two models differed notably with respect to the dominating drivers and underlying processes. Fire-vegetation interactions and socioeconomic effects emerged as important uncertainties for future burned area in some European regions. Burned area of eastern Europe increased in both models, pointing at an emerging new fire-prone region that should gain further attention for future fire management.

1. Introduction

Wildland fires are a worldwide phenomenon and play an important role for ecosystems through affecting biogeochemical cycles and biogeophysical properties [*Bowman et al.*, 2009]. Fire has influenced the Earth System over hundreds of millions of years, but changes in fire regimes have been documented best since the last ice age [*Marlon et al.*, 2008; *Daniau et al.*, 2010]. From an atmospheric perspective, fire-related emissions from biomass burning influence the concentration of greenhouse gases in the atmosphere as well as short-lived, reactive substances, but the overall effects on radiative forcing are uncertain [*Ciais et al.*, 2013]. Fire also leads to changes in vegetation cover and thus affects surface properties [*Randerson et al.*, 2006]. Regular occurrence of fire is also an important component that affects vegetation structure and species composition [*Bowman and Panton*, 1995; *Moreira*, 2000; *Shackleton and Scholes*, 2000; *Bond et al.*, 2005].

Fire is affected by biotic and abiotic factors such as weather and fuel (type, load, continuity, and structure). For example, grass-dominated fuel types tend to accelerate fire spread [*Johnson*, 1992; *Flannigan et al.*, 2000; *Flannigan et al.*, 2005; *Westerling et al.*, 2006; *van der Werf et al.*, 2008] compared to more coarse, woody fuels. But fire is also strongly controlled by socioeconomic factors. Throughout history, human activities have increasingly been influencing fire regimes through population growth, settlements, changes in land use, and fire management [*Savage and Swetnam*, 1990; *Guyette et al.*, 2002; *Mouillot and Field*, 2005; *Marlon et al.*, 2008; *McWethy et al.*, 2010; *Roebroeks and Villa*, 2011]. Since in addition to climate change and increasing atmospheric CO_2 concentrations, demography and human land use are projected to continue to change in the future, it poses the question of how these factors will interact and drive changes in future fire regimes regionally.

In Europe, with on average half a million hectares of area burned every year [*Camia et al.*, 2010; *Schmuck et al.*, 2011], 85% of the total occur in Mediterranean Europe [*Schmuck et al.*, 2011]. Fire is considered to cause large

ecosystem and socioeconomic losses [*San-Miguel-Ayanz et al.*, 2013]. Presently, more than 90% of the fires in Europe are caused by humans [*Ganteaume et al.*, 2013], and some can result in very large fire events with associated damage to human properties and lives. But "natural" fire regimes in many parts of Europe are difficult to quantify given Europe's long history of human land use, which makes it difficult to judge how present fire regimes would differ from a Europe without humans. Fire regimes in Europe are not only affected by human ignition [*Ganteaume et al.*, 2013] but also by fire management [*Moreira et al.*, 2011], which complicates the assessment of the overall anthropogenic effects on burned area—at continental and subcontinental scales.

Future fire activity in Europe is expected to increase due to enhanced occurrence of fire-prone weather conditions, and climate has been identified as a main driver for future fire regimes [*Mouillot et al.*, 2002; *Moriondo et al.*, 2006; *Amatulli et al.*, 2013]. Recent studies have included human effects and these have reported a dampening of the climate effects on fire emissions [e.g., *Kloster et al.*, 2012; *Migliavacca et al.*, 2013b]. Moreover, atmospheric CO_2 fertilization has so far only been investigated for effects on vegetation through enhancing photosynthesis and water use efficiency [*Cramer et al.*, 2001; *Hickler et al.*, 2008; *Sun et al.*, 2014], while its indirect impact on fire has not yet been explicitly quantified. Filling this gap by quantifying the potential effect of CO_2 fertilization could be helpful to understand future fire regimes for Europe. In addition, future burned area has been so far mainly investigated in the context of fire emission projections, but no study has specifically addressed and systematically investigated how global environmental change would affect burned area across Europe. Since burned area also has a large impact on human societies, by destroying properties and endangering lives, this aspect of fire regimes deserves more attention.

In this study, we address the question of how CO_2 fertilization and human population density influence future burned area in Europe compared to the effects of climate change. To enable the exploration of potential sensitivities, we conducted a series of factorial experiments to evaluate the influence of climatic, physiological, and socioeconomic conditions on future fire regimes separately. We applied two integrated fire-vegetation models: LPJ-GUESS coupled with the empirical fire submodel SIMFIRE and LPJmL coupled with the process-based fire submodel SPITFIRE, driven by climate data from four CMIP5 Earth System Models (ESMs) and two different Representative Concentration Pathways (RCPs), which were combined with two Shared Socioeconomic Pathways (SSPs).

2. Materials and Methods

2.1. Common Features in Two Models

The two integrated fire-vegetation models, LPJ-GUESS-SIMFIRE and LPJmL-SPITFIRE, used in this study share certain features with the Lund-Potsdam-Jena Dynamic Global Vegetation Model [LPJ-DGVM,*Sitch et al.*, 2003]: physiological processes like the calculation of carbon fluxes (gross primary production and autotrophic and heterotrophic respiration) and pools (in leaves, sapwood, heartwood, storage organs, roots, litter, and soil), as well as water fluxes (interception, evaporation, transpiration, soil moisture, snowmelt, and runoff). Carbon and water dynamics are closely linked through canopy conductance and are simulated on a daily time step in response to changing temperatures, declining water availability and rising atmospheric CO_2 concentrations. Meanwhile, the two models maintain also very unique features described in the following.

2.2. LPJ-GUESS-SIMFIRE

The dynamic vegetation submodel, LPJ-GUESS in LPJ-GUESS-SIMFIRE, is designed for regional to global applications, especially regarding forest-gap model approaches in simulation of vegetation dynamics [*Smith et al.*, 2001]. LPJ-GUESS simulates growth dynamics of age cohorts. Stochastic growth, mortality events, and disturbance in vegetation are represented by averaging multiple simulated patches for a given location (grid cell). Each patch with separated stochastic events hosts a mixture of plant functional types (PFTs), and each PFT per patch is represented by one mean individual. We applied the model following the Europe-specific PFT setting used by *Hickler et al.* [2012], with 14 different tree PFTs, 4 shrub PFTs, and two herbaceous PFTs (one for C_3 and one for C_4 photosynthesis, respectively). Establishment and mortality are influenced by resource competition.

SIMFIRE predicts annual burned area on the basis of biome type and fuel continuity (determined from vegetation characteristics simulated by LPJ-GUESS), climatic fire danger (defined as the probability of burning

from climate forcing), and human population density (provided as external forcing). A limited set of global parameters were derived by inversion of SIMFIRE against global multiyear satellite-observed burned area [*Knorr et al.*, 2014]. When using only European burned area data for the optimization, it was not possible to find a satisfactory minimum. Therefore, in order to adjust certain parameters to represent conditions in Europe as closely as possible, we set up a regionalized parameterization using socioeconomic regions in combination with biomes as described by *Knorr et al.* [2014] (see Table A2 and Figure B2 therein for the socioeconomic regions, including Europe). In this setup, a biome is split into different parts according to the socioeconomic region in which it is located, and each part is treated effectively as a separate "biome." For this study, the following biomes were differentiated by socioeconomic region: "cropland/urban/natural vegetation mosaic," "shrubland," "savanna or grassland," "needleleaf forest," and "tundra," resulting in 36 regions overall. For the coupled runs of LPJ-GUESS and SIMFIRE, for those aforementioned biomes that had been split by socioeconomic regions we used the parameter values associated with the region "Europe," while the remaining biomes had only one global parameter value, which we used here (see Table S1).

The biome type in SIMFIRE directly influences burned area. When SIMFIRE is coupled to LPJ-GUESS, it is computed based on the percentage of woody PFTs (to distinguish grasslands) and vegetation height (to distinguish shrubs from trees), and the fraction of tropical versus extratropical PFTs. Climatic fire danger is represented by the maximum daily Nesterov index [*Thonicke et al.*, 2010] during a fire year, computed for each grid cell according to the local weather (input from the external forcing data). Fuel continuity is estimated from the annual maximum vegetation fraction of absorbed photosynthetically active radiation (FAPAR) simulated by LPJ-GUESS. The impacts of fire on carbon emissions and plant litter dynamics are implemented as described by *Knorr et al.* [2012]. For further details on SIMFIRE see *Knorr et al.* [2014], while its coupling with LPJ-GUESS is described in *Knorr et al.* [2015].

Total burned area can be significantly influenced by small fires, here meant as those fires below the resolution of surface reflectance imagery used to map burn scars in global burned area products, i.e., between 21 ha and approximately 100 ha [*Randerson et al.*, 2012]. These fires often occur in agricultural land [*McCarty et al.*, 2009]. However, optimization of SIMFIRE taking into account small fires led to rather similar parameters to one without a small-fire correction [*Knorr et al.*, 2014]. Therefore, with the focus of this study on natural vegetation and given that the correction for small fires is also uncertain, we applied LPJ-GUESS-SIMFIRE with fire risk parameters optimized based on GFED3.1, which does not account for small fires.

2.3. LPJmL-SPITFIRE

The dynamic vegetation submodel LPJmL (The Lund-Potsdam-Jena dynamic global vegetation model for managed land) in LPJmL-SPITFIRE considers dynamic land management and describes vegetation dynamics as driven by climate and soil conditions. Natural vegetation is represented at the biome level by nine plant functional types [*Sitch et al.*, 2003], and growth, phenology, and harvest of 12 crop functional types accounts for agricultural production [*Bondeau et al.*, 2007]. Area-based approaches are applied and no gap model features or age cohorts are implemented, but at each location, one average individual per PFT growing at this location is simulated.

Fire is simulated using the process-based fire model SPITFIRE [*Thonicke et al.*, 2010], which calculates climatic fire danger, human- and lightning-caused ignitions as well as spread, effects, and emissions of fire. SPITFIRE simulates small- to large-scale fires as long as the minimum fire-line intensity provides enough energy for the fires to spread. Area burned can be limited by low-climatic fire danger as it limits fire duration, and by fuel availability as it limits fire spread. Regionally specific fire ignition pattern are based on the parameterization approach for human-caused fires derived from relatively precise and robust long-term fire statistics including small burned area for the Mediterranean region [*Moreno et al.*, 1998] and European temperate forest [*Thonicke and Cramer*, 2006]. This process-based fire model allows for investigating changes in human population density on fire ignitions, changes in vegetation productivity, or changes in fuel size on fire spread, as well as feedback to vegetation by fuel combustion and postfire mortality. Postfire mortalities for PFTs are determined based on the amount of damage to the crown, and to the cambium, both of which are relevant to the simulated fire intensity.

2.4. Input Data

Both vegetation models were forced by the same temperature, precipitation, solar radiation, atmospheric CO_2 concentration, and human population density from 1901 to 2100 (supporting information Figure S1).

Table 1. Overview of Scenario Combinations and CMIP5 Models Used in This Study[a]

Scenarios Name	Model Name	Greenhouse Gas Scenario	Population Scenario
MPI85	MPI-ESM-LR[b]	RCP 8.5	SSP5
MPI26	MPI-ESM-LR[b]	RCP 2.6	SSP1
IPSL85	IPSL-CM5A-MR[c]	RCP 8.5	SSP5
IPSL26	IPSL-CM5A-MR[c]	RCP 2.6	SSP1
HAD85	HadGEM2-ES[d]	RCP 8.5	SSP5
HAD26	HadGEM2-ES[d]	RCP 2.6	SSP1
CCSM85	CCSM4[e]	RCP 8.5	SSP5
CCSM26	CCSM4[e]	RCP 2.6	SSP1

[a]The succeeding footnotes are the names of the modeling center for each model.
[b]Max Planck Institute for Meteorology.
[c]Institut Pierre-Simon Laplace.
[d]Met Office Hadley Centre.
[e]National Center for Atmospheric Research.

LPJmL-SPITFIRE additionally requires wind speed data to calculate fire spread. We used climate model simulations from the CMIP5 project [*Taylor et al.*, 2012] based on the Representative Concentrations Pathways (RCPs) 2.6 and 8.5 [*van Vuuren et al.*, 2011] from four ESMs (Table 1). Monthly output from the ESM simulations was interpolated to a $0.5 \times 0.5°$ grid resolution and bias corrected against the mean climate of 1961–1990 derived from Climatic Research Unit Timeseries 3.10 [*Harris et al.*, 2014] in a way mostly following [*Ahlström et al.*, 2012], in which climate output of monthly mean temperature and shortwave radiation were linearly interpolated to daily values, and daily precipitation was simulated by a weather generator based on monthly fraction of rain days. In addition, we followed the approach by *Knorr et al.* [2015] to predict the monthly number of rainy days and the monthly mean diurnal temperature for future based on linear regressions against monthly mean precipitation and temperature, respectively. Atmospheric CO_2 concentrations were taken directly from corresponding scenarios RCP 8.5 and RCP 2.6 (Figure S1b).

Population data were used from the historical estimates of History Database of the Global Environment (HYDE) 3.1 [*Goldewijk et al.*, 2010] aggregated to 0.5° by 0.5° spatial resolution until the year 2005. For future projections, population scenarios SSP1 and SSP5 under the framework of SSPs [*O'Neill et al.*, 2014] were used (https://secure.iiasa.ac.at/web-apps/ene/SspDb/dsd?Action=htmlpage&page=about; Table 1). SSP1 assumes a sustainable development directed toward environmentally friendly processes with low carbon emission and low population growth rates, and SSP5 assumes the absence of climate policies with rapid economic development, high carbon emission and high population growth rates [*O'Neill et al.*, 2014]. Both SSP1 and SSP5 use the same fast urbanization scenario [*Jiang*, 2014]. In our study, we applied the combination of RCP 2.6 with SSP1, and RCP 8.5 with SSP5, following recommendations from *van Vuuren and Carter* [2014]. The SSP population scenarios with changes in population in urban regions, which were available on a per-country basis, were applied to the spatial distribution of HYDE 3.1 for 2005. To do so, the rural and urban populations of HYDE were multiplied separately for each country by the population growth relative to 2005, followed by a rescaling of the population density for all grid cells of each country to match the per-country values again. LPJmL-SPITFIRE additionally used historical land use data to restrict the size of the potential burned area and to account for large-scale landscape fragmentation [*Fader et al.*, 2011]. By subdividing the grid cell into a stand, where natural vegetation was simulated, and several other stands, where the growth dynamics of crops and managed grassland were simulated. The size of the natural stand determines the maximum size of area burned in natural vegetation, i.e., wildfires.

2.5. Simulation Experiments

The simulation experiments were initialized with a 300 year spin-up period using detrended climate from the ESMs for the years 1901 to 1920 repeated 15 times, during which constant atmospheric CO_2 concentration and constant human population density of the year 1900 were used. In addition, LPJmL-SPITFIRE used a fixed land use fraction for the year 1900 for an additional land use spin-up to bring carbon and water pools into equilibrium with early land use conditions. Land use restriction in LPJ-GUESS-SIMFIRE was not turned on in the simulation but was considered in the analyses (see section 2.6). After spin-up, for the years 1901 to 2000, both models were driven by historical CO_2 concentrations taken from the RCP data set, the historical human population density estimates from HYDE 3.1 and climate input data from the bias corrected CMIP5

Table 2. Overview of Factorial Experiments for Each Scenario as Shown in Table 1[a]

Experiment	Climate	CO_2	Population Density	Effects Derived for Analysis
FUL_EFF	+	+	+	Full effect
CON_POP	+	+	–	Population effect = FUL_EFF – CON_POP
CON_CO2	+	-	+	CO_2 effect = FUL_EFF – CON_CO2
CON_CLM	–[b]	+	+	Climate effect = FUL_EFF – CON_CLM

[a]+: input data follow scenarios. –: input data remain constant after 2000.
[b]After 2000 input is detrended climate data from 1981 to 2000 repeated every 20 years.

simulations. The land use fraction used in LPJmL-SPITFIRE was changing until the year 2001 but was kept constant thereafter. From 2001 onward, forcing data from climate and atmospheric CO_2 scenarios based on the RCPs and population scenarios based on SSPs were applied for the standard experiments. For factorial experiments, we used various combinations of scenarios as detailed in Table 2.

In the standard experiments (FUL_EFF, "full effect," see Table 2), all external drivers were allowed to change. The factorial experiments followed the FUL_EFF simulation until 2000, after which one external driver (climate, atmospheric CO_2, or human population density) was kept constant in order to estimate its marginal effect on the overall outcome in the future. In the CON_CLM ("constant climate") experiment, a 20 year detrended climate forcing based on the period 1981–2000 was repeated five times from 2001 until 2100. For the CON_CO2 ("constant CO_2") and CON_POP ("constant population") experiments, atmospheric CO_2 concentration and human population density, respectively, were kept constant at the level of the year 2000 throughout the 21st century.

The impacts of nitrogen (N) cycle on vegetation growth are not included in the model versions adopted in this study.

2.6. Methods of Analysis

The marginal effects of factors were estimated by the comparison between the FUL_EFF and each factorial simulation experiment (Table 2).We based our analysis for factorial effects on relative changes of simulated future burned area compared to the present, i.e., the factorial effect for the variable concerned can be represented as the Relative Factorial Effect (RFE) of variable Λ for a specific time period, calculated as follows:

$$\mathrm{RFE} = \left(\Lambda_{\mathrm{F,\ future}} - \Lambda_{\mathrm{X,\ future}}\right) / \Lambda_{\mathrm{F,\ present}} \quad (1)$$

$\Lambda_{\mathrm{F,\ future}}$ is the value from the FUL_EFF experiment for the future (2081–2100), Λ_{X} the same variable from one of the factorial experiments for the same future period (with X representing either CON_CLIM, CON_CO2, or CON_POP), and $\Lambda_{\mathrm{F,\ present}}$ the value taken from the FUL_EFF experiment during the recent reference period (1981–2000). The relative factorial effects for climate change, CO_2 fertilization, and population density thus are denoted as $\mathrm{RFE_{CC}}$, $\mathrm{RFE_{CO2}}$, and $\mathrm{RFE_{PD}}$, respectively. We employed the Mann-Whitney *U* test, a nonparametric testing approach to indicate significant changes in simulations compared to each grid cell separately within specific time series. This test does not require the assumption of a normal distribution of the underlying statistical populations [*Hollander and Wolfe*, 1999] and filters "noise" that may lead to misinterpretation of changes in spatial pattern.

As we focus on changes in wildfires in Europe, but not on agricultural activities such as agricultural clearing and stubble burning, we excluded from the analysis grid cells with more than 50% agricultural land using data from the year 2005 by *Ramankutty and Foley* [1999]. Results are presented on the basis of ensemble means except for Figures 5 and 6, in which MPI-ESM-LR is chosen as an example to illustrate factorial impacts on spatial changes in burned area. Total and regional burned areas in the simulations with MPI-ESM were closest to the ensemble mean and therefore considered most representative. In the following text, LPJ-GUESS-SIMFIRE and LPJmL-SPITFIRE are denoted as "LPJ-GUESS" and "LPJmL," respectively, unless otherwise specified. All simulations were conducted for a domain covering Europe expanding from 15°W to 38°E and 35°S and 72°N, and results are presented for the entire domain as well as for the following subregions (see Figure S2 for definition): Mediterranean Europe, eastern Europe, western Europe, and northern Europe. The extension of each subregion was adjusted according to the availability of evaluation data for administrative units.

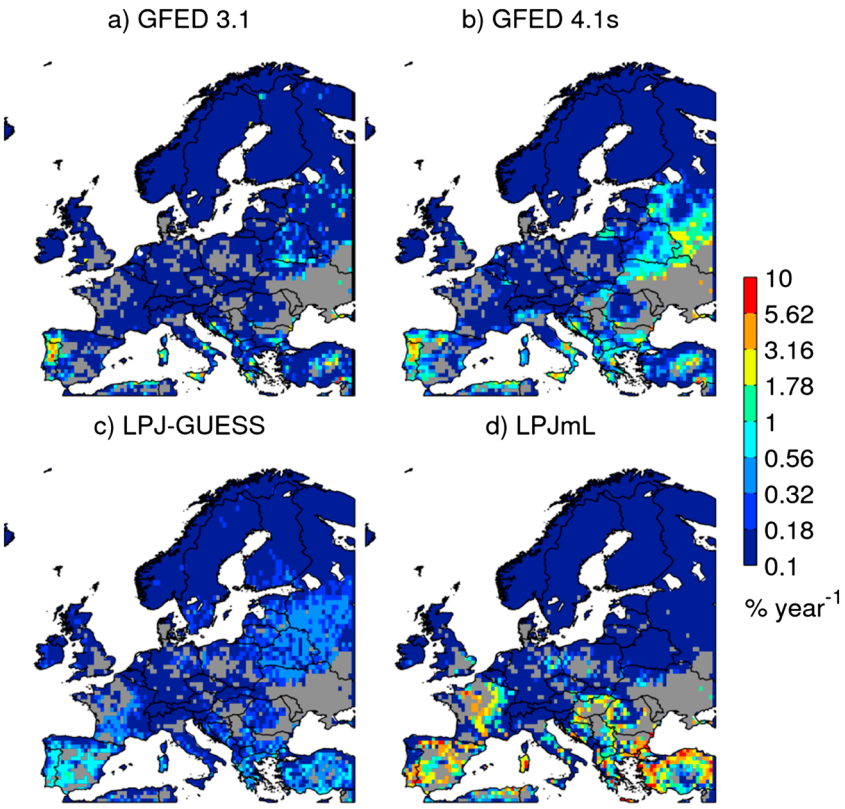

Figure 1. Observed ((a) GFED 3.1 and (b) GFED 4.1 s) versus simulated (c and d) mean annual burned fraction for Europe over the period 1997–2009. Figures 1c and 1d are from the ensemble mean of ESMs-driven simulations (Table 1) in experiment FUL_EFF (Table 2). Areas with greater than 50% agricultural land were excluded (grey).

3. Results

3.1. Model Evaluation

We evaluated the spatial and temporal patterns of the cross-ESM ensemble mean burned area by the two models against monthly burned area from the Global Fire Emission Database, GFED3.1 (Figure 1a) [*Giglio et al.*, 2010] which is calculated from multisatellite products, gridded to 0.5° spatial resolution and available for the time period July 1996 through February 2012. In addition, the recently released GFED 4.1 s is also shown, which includes the effect of small fires and covers a longer time period (1997–2014; Figure 1b) [*Randerson et al.*, 2012]. Furthermore, we compared simulation results against monthly burned area data from the European Fire Database [*Camia et al.*, 2010] of the European Forest Fire Information System (EFFIS; http://effis.jrc.ec.europa.eu) which is based on regional administrative statistics of reported burned area in natural vegetation (Figure 2). The period 1997–2009 with full annual burned area cycles was chosen as the evaluation period.

At the continental scale, the spatial patterns are generally comparable between the two vegetation-fire models and observation-based estimates (Figures 1 and 2). Simulated burned area of LPJ-GUESS is around 0.38 Mha/yr for the Mediterranean region, in closer agreement with GFED 3.1, which does not include small fires. Overall, LPJ-GUESS, GFED 3.1, and EFFIS are showing a burned area in the order of 0.42 Mha/yr for this region. LPJ-GUESS generally overestimated burned area for the rest of the continent, but the simulated total burned area in Europe outside the Mediterranean was very small (Figures 1 and 2). With considering small fires, GFED4.1 s shows around 50% increase in burned area for the Mediterranean and also differs for the rest of continent compared with GFED 3.1. For Mediterranean Europe, the burned area is more comparable with LPJmL, which distinguishes small fires and generally simulated more fire activity for Europe. For eastern Europe, both LPJ-GUESS and LPJmL compare better with the more recent GFED product.

In addition to the spatial patterns, we compared the time series in burned area for the major wildfire countries in the Mediterranean region (Figure 3) as well as for the rest of regions in Europe (Figure S3). A small

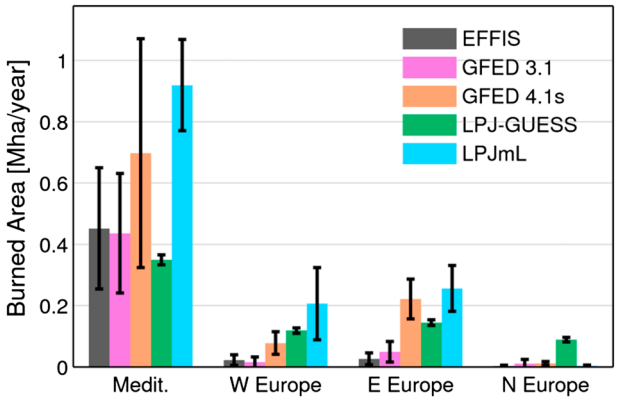

Figure 2. Observation-based (EFFIS, GFED 3.1, and GFED 4.1 s) versus simulated annual burned area for four European regions. The bar and the range represent the mean and the standard deviation of burned area over the period 1997–2009. Simulated burned area is calculated based on the ensemble mean of ESMs-driven simulations (Table 1) in experiment FUL_EFF (Table 2). Areas with greater than 50% agricultural land were excluded from the calculation. Regions are defined in Figure S2.

declining tendency was observed in all three observation-based products. LPJ-GUESS simulated declining trends both at regional and country level with comparable variability. These simulated trends across the Mediterranean region and for Europe generally reflect the observations, though deviations exist for some regions and countries (e.g., Italy). Simulated trends from LPJmL were overall similar to those found for LPJ-GUESS for many countries and regions. However, the model presents small positive trends when run for Europe as a whole, as well as for the Mediterranean. These were mainly influenced by a mismatch in Spain with overestimated fires toward the end of the simulation period. For other regions, the two models overall can capture variability satisfactorily especially for eastern Europe.

3.2. Future Change in Burned Area

The combined effect of climate, atmospheric CO_2, and human population density on future burned area for Europe, based on the experiment FUL_EFF, showed an increase over the 21st century for both models, leading to a considerably larger burned area by 2100 (Figure 4). The overall changes in the RCP8.5-SSP5 scenario were around 1.8 (for LPJ-GUESS) and 3.6 (for LPJmL) times the present-day values (Figure 4). Simulations with RCP2.6-SSP1 led to a more moderate change, with less than 60% increase for both models, and the difference between the two models was much smaller. Simulated burned areas under the two RCPs start to deviate differently for the two models, around 2025 (LPJmL) and around 2040 (LPJ-GUESS). The differences in simulated burned area can partly be explained by underlying simulated changes in vegetation composition. While

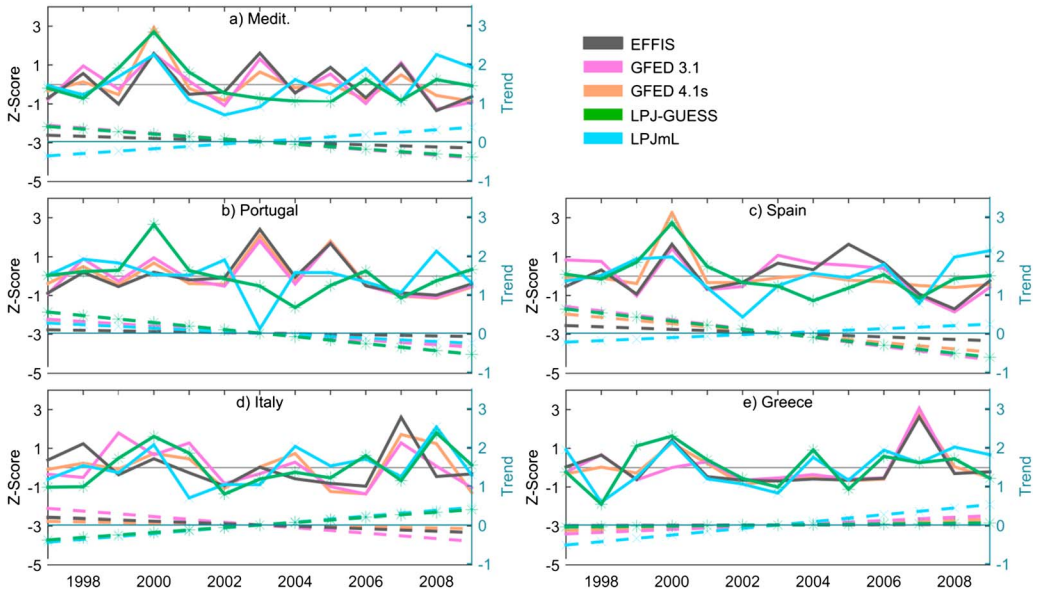

Figure 3. Trends (dashed line) and variability (solid line) of observed and simulated burned area for countries in the Mediterranean region where wildfires are prominent over the period 1997–2009. Simulated burned area is calculated based on the ensemble mean of ESMs-driven simulations (Table 1) in experiment FUL_EFF (Table 2). The variability and trend are calculated based on the *Z*-scores of the observed and simulated cross-ESMs ensemble mean annual burned area.

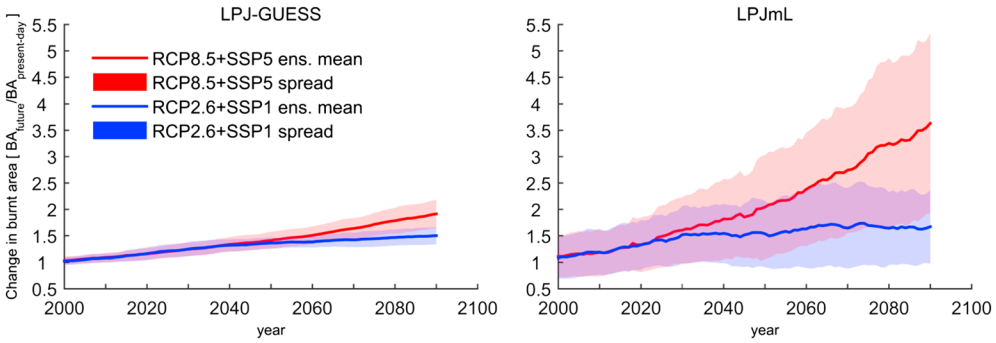

Figure 4. Simulated relative changes in burned area (BA) for Europe to the end of 21st century by two models, represented as ensemble relative change to present date (1981–2000) for four ESMs in RCP 8.5 and RCP 2.6 scenarios ($BA_{future}/BA_{present\text{-}day}$). Spreads are ESMs uncertainties represented as one standard deviation among ESMs from the ensemble mean. All lines are smoothed with 20 year moving average.

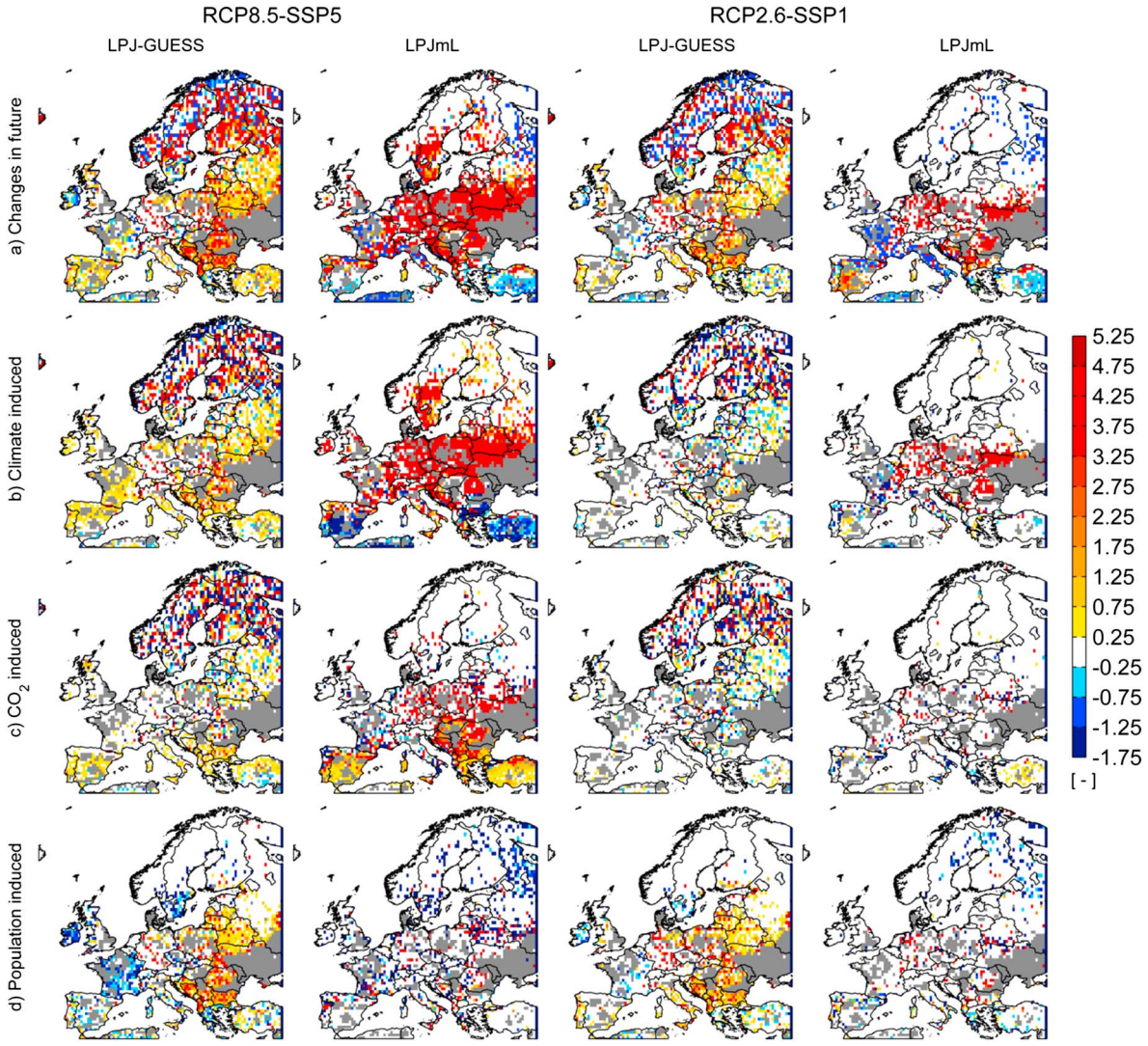

Figure 5. Changes in mean annual burned fraction (BF) in MPI-ESM-LR simulations related to present date. (a) Relative changes between future (2081–2100) and present date (1981–2000) in experiments FUL_EFF ($BF_{future}/BF_{present\text{-}day} - 1$); (b to d) Relative factorial effect (RFE, equation (1) and Table 2) for annual burned area fraction in future. Only significant changes ($p < 0.05$) are presented using Mann-Whitney *U* test. Areas with no change or nonsignificant change are in white. Areas with greater than 50% agricultural land were excluded (grey).

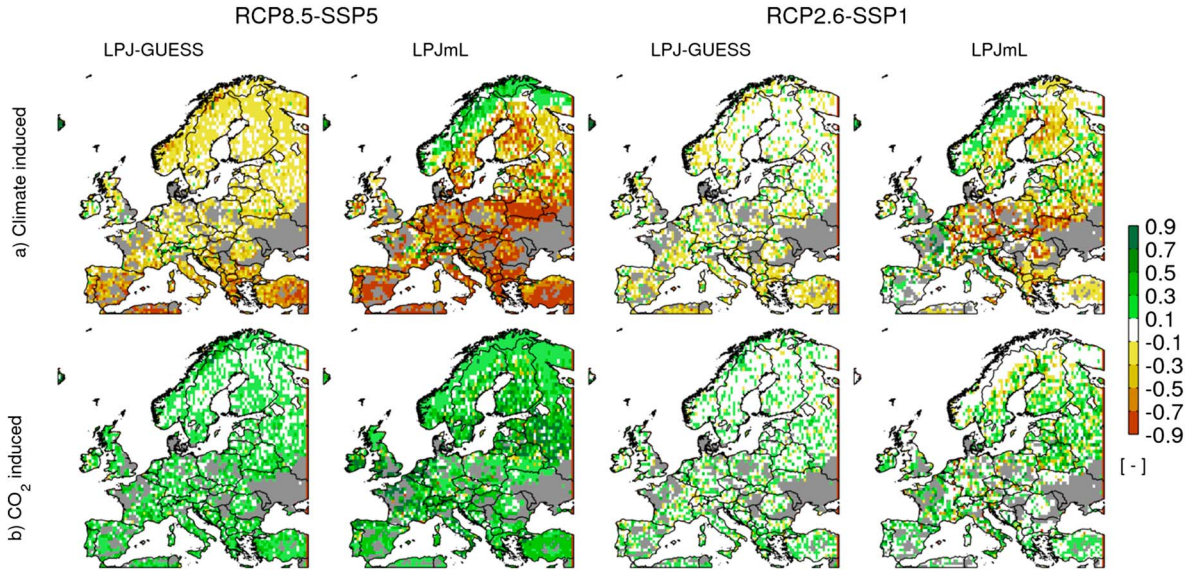

Figure 6. Relative factorial effects (RFE, equation (1) and Table 2) for fuel load represented as the sum of aboveground biomass and litter due to changes in climate and atmospheric CO_2 concentration. Results are from MPI-ESM-LR, only significant changes ($p < 0.05$) between FUL_EFF and correspondent factorial experiments in future (2081–2100) are presented using Mann-Whitney *U* test. Areas with no change or nonsignificant change are in white. Areas with greater than 50% agricultural land were excluded (grey).

LPJ-GUESS simulates relatively small vegetation changes, herbaceous vegetation is gaining dominance in LPJmL (Figure S4).

While both models project a strong increase in burned area at the continental scale, the spatial patterns were only in parts comparable (e.g., increase in burned area in eastern and parts of northern Europe and parts of Mediterranean Europe; Figure 5a, represented as change in mean annual burned fraction, i.e., change in the probability of a pixel being burnt per year). The RCP8.5-SSP5 and RCP2.6-SSP1 simulations differed not only in the magnitude of the changes (Figure 4) but also in the direction of change in different regions (Figure 5a).

3.3. Climate Effects

Climate change affects the occurrence of hot temperatures and soil moisture deficits and thus changes climatic fire danger but has also indirect effects through impacts on vegetation productivity and thereby changing fuel buildup (Figure 6). When focusing on climate alone, both models simulated a positive climate effect on fire across most of Europe, but with, as expected, burned-area responses to the RCP8.5-SSP5 forcing being much higher than for RCP2.6-SSP1 (Figure 5b). When aggregated for the subregions (Figure 7), climate-response trends were found to be similar in LPJ-GUESS and LPJmL for most regions. Increases in burned area were mainly caused by a direct climate effect, that is, increase in climatic fire danger at higher temperature (approximately +4°K, Figure S5a) and/or decrease in precipitation (approximately −100 mm/yr, Figure S5b) outweighed the negative climate effects on vegetation productivity and fuel load (Figure 6a) in both models.

The two models differed, however, in their projected trends for Mediterranean Europe (especially for the RCP8.5 scenario, Figure 7): Similar to other subregions, LPJ-GUESS simulated an increase in burned area for the RCP8.5-SSP5 scenario (RFE_{CC} is +37%, Table S2), as the increase in climatic fire danger in LPJ-GUESS overrode the slightly negative effect of climate change on fuel load (Figure 6), leading to a considerable increase in absolute burned area (Table S2). By contrast, LPJmL simulated a declining burned area for Mediterranean Europe in the RCP8.5 runs, especially in parts of the Iberian Peninsula (and more or less no change in RCP2.6; Figures 5 and 7; −76%,Table S2). The strongly declining fuel load in this region (Figure 6) posed a fuel limitation sufficient to limit fire spread. In all other regions, climate change led to either a strong increase in burned area in simulations with both models (RCP8.5), or little to no change (RCP2.6; Figures 5 and 7).

3.4. Atmospheric CO_2 Effects

Atmospheric CO_2 concentration is projected to reach 936 ppmv for RCP85 and 421 ppmv for RCP2.6 by the end of 21st century (Figure S1b). The enhanced atmospheric CO_2 concentration (compared to 369 ppmv in

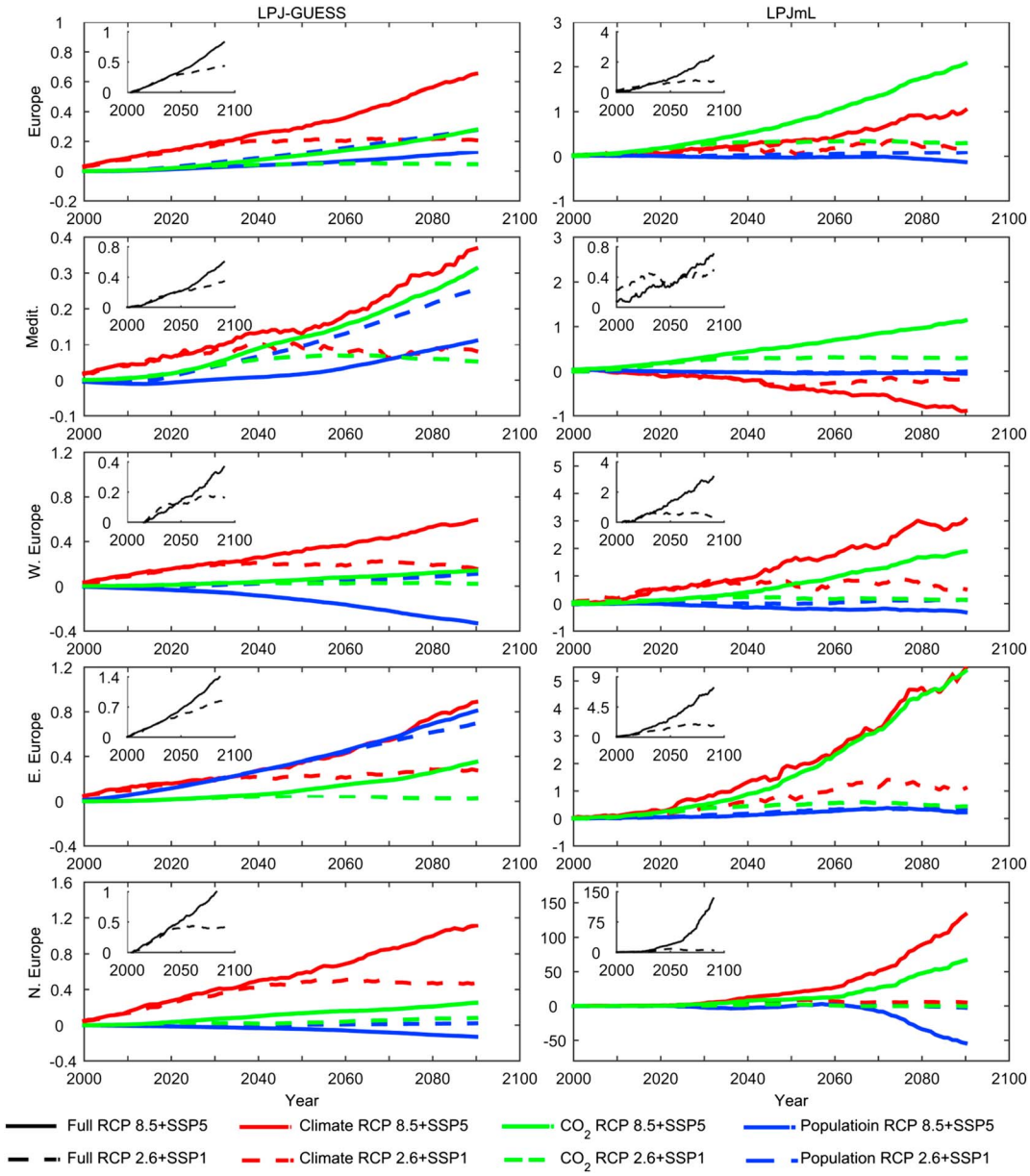

Figure 7. Relative factorial effect (RFE, equation (1) and Table 2) of climate, atmospheric CO_2, and human population density to annual burned area over time in regions under different scenarios, represented as ensemble changes between FUL_EFF and factorial experiments relative to the mean of present date; inset plots are relative changes in burned area represented as $BA_{future}/BA_{present\text{-}day} - 1$. RFE for northern Europe for LPJmL are relatively large due to very low fire simulated for present date. Areas with greater than 50% agricultural land were excluded from the calculation. All lines are smoothed with 20 year moving average. Please note the different *y* axis.

CON_CO2) in the future resulted in a general increase in fuel load by approximately 10%–70% for Europe (Figure 6). In response to this increase in fuel load, both models simulated a general increase in burned area, by 30% for LPJ-GUESS, and by 223% for LPJmL for Europe in the high-CO_2, RCP8.5-SSP5 scenario (Figures 5 and 7). At the European scale, the CO_2 effects hence outweighed the climate-change effects in burned area in LPJmL, while for LPJ-GUESS, climate change was the more important driver (Figure 7). A similar response in LPJ-GUESS was also found in the RCP2.6 simulations, while for RCP2.6 in LPJmL, the climate change and CO_2 effects were approximately similar when averaged across the continent.

Regionally, effects of CO_2 (in the RCP8.5 scenario) were quite pronounced in Mediterranean Europe for both models, and parts of eastern Europe (Figures 5 and 7), mirroring the spatial patterns of the CO_2 effects on

vegetation productivity and fuel load to some degree (Figure 6). Beside influences from changes in fuel load, changes in burned area also reflected changes in the actual vegetation type. Negative RFE_{CO2} were simulated by LPJ-GUESS (Figure 5) for the area where changes in biome type (not shown) and woody-grass ratio (Figure S4) also happened, though given a general increase in fuel load. By contrast, LPJmL simulated an increase in fuel load and relatively stable vegetation composition (albeit much different compared to LPJ-GUESS; Figures 6 and S4) therefore providing enough fuel and contributing even a greater effect for the increase in burned area for the whole Europe (Figure 7, "Europe").

3.5. Population Effects

In both future scenarios population density increases for Europe until the mid-21st century, after which population growth continues for SSP5, while population drops again to approximately present-day values for SSP1 (Figure S1). Meanwhile, the urban share of the European population increases in both future scenarios through the end of 21st century with faster rates for eastern Europe than other regions (https://secure.iiasa.ac.at/web-apps/ene/SspDb/dsd?Action=htmlpage&page=countries). Southern Scandinavia and western Europe are projected to be the main population-increasing regions, while population in eastern Europe is projected to decline for both SSPs (Figure S5). In SSP5 a strong regional divergence between eastern and (north) western Europe emerges, while in SSP1 at the end of the 21st century a decline is also projected for parts of central and Mediterranean Europe. For burned area, at the European scale, the overall population effects in RCP8.5 were nearly negligible (Figure 7, $RFE_{PD} < 0.2$), but for RCP2.6 burned area in LPJ-GUESS increased with population change, and the total effect was even larger than the simulated climate effect. By contrast, population change did not impact burned area (or had even negative RFE_{PD}) in LPJmL in the RCP2.6 runs. At the subregion scale, the effect of population density in LPJ-GUESS was on a par with the effect of climate change for eastern Europe in RCP8.5, and substantial differences between the two RCPs emerged (e.g., Mediterranean, western Europe). In LPJmL effects of population were least important of the three investigated drivers in all subregions, with exception of northern Europe, and no difference between the RCP8.5 and 2.6 scenarios emerged (Figure 7).

4. Discussion

4.1. Temporal Trends at the European Level

Few studies so far have, in addition to climate change, investigated effects of vegetation and socioeconomic changes on wildfires, and the effects of these additional important drivers atop of climate change are so far very uncertain [*Kloster et al.*, 2012; *Migliavacca et al.*, 2013b]. For example, *Migliavacca et al.* [2013b] simulated a stronger impact of human fire suppression, and a weaker fuel load effect on changes in fire emissions for Europe by the end of the 21st century compared to a study by *Kloster et al.* [2012].

In transient future simulations, the two models projected increasing burned area on the continental scale, with very different overall magnitude under the severe RCP8.5 scenario but similar increase under RCP2.6 (Figure 7). In LPJ-GUESS, the impact of climate change on burned area was the overall dominating effect followed by atmospheric CO_2 and human effects, all contributing to the increase in future burned area. In LPJmL, positive effects by CO_2 on fuel load were very strong, and CO_2 emerged as the continentally dominating effect. The previous study by *Migliavacca et al.* [2013b] estimated a less than 15% increase in burned area for Europe by the end of the 21st century under the Special Report on Emissions Scenario A1B scenario, with a dominant climate effect (as in LPJ-GUESS) and a negative human effect (as in LPJmL). The dominating effects are comparable to our findings, but the scale of increase in future burned area for the continent was much smaller by comparison (15% versus 88% for LPJ-GUESS, 265% for LPJmL, see Table S2). Apart from the different climate scenarios used, this difference may be partly caused by the different sensitivity of fire-vegetation interactions in the models applied. The fire algorithm in *Migliavacca et al.* [2013a] puts an upper limit on fuel influencing fire probability and additionally simulates fire suppression effects, such mechanisms are not incorporated in the two fire models used here. In addition, the difference may be also partly caused by the consideration of small fires and the associated uncertainties implied by the correction procedure in the observation. The difference EFFIS minus GFED3.1 differs considerably from GFED4.1 s minus GFED3.1, even though both EFFIS and GFED4.1 s include small fires (Figure 2). It should also be considered that *Migliavacca et al.* [2013a] calibrated their model against EFFIS, and not GFED4.1 s, which has only become available recently. The 15% increase in *Migliavacca et al.* [2013b] can be regarded as the more conservative

estimation, while our results in this study represent a high-impact potential future. Similar to our results, *Migliavacca et al.* [2013b] also found increasing burned area for eastern Europe, but a more quantitative discussion of the different contributing factors is difficult due to the differences in experiment setup and analysis.

4.2. Eastern Europe: A Potential New Fire-Prone Area

Over the last decades, an increasing trend in burned area has been observed for eastern Europe [*Schmuck et al.*, 2014]. Our study showed a considerable increase in burned area in the future, a trend that corresponds with previously simulated increases in fires activity [*Krawchuk et al.*, 2009; *Pechony and Shindell*, 2010] and in fire emissions [*Kloster et al.*, 2012; *Migliavacca et al.*, 2013b; *Knorr et al.*, 2015] for the same region. These studies, however, have attributed changes in fire activity and emissions to different processes. For example, the increase in fire numbers in eastern Europe projected by *Krawchuk et al.* [2009] was explained mainly by climate change alone. Their study was based on statistical models that linked fire activity to a number of drivers, including interactions of climate change and net primary production. Vegetation effects were small for eastern Europe as interactions between vegetation composition through fuel load, tree architecture, or the proportion of fine fuel and fire were not considered. Using a coupled fire-vegetation-biogeochemical model, *Kloster et al.* [2012] and *Migliavacca et al.* [2013b] simulated an increase in fire emissions for eastern Europe and also attributed the increase mostly to climate change when explicitly considering other drivers such as aboveground biomass and population density. Such increasing trend for eastern Europe is in agreement with the recent global simulation study by *Knorr et al.* [2015] which found highly significant increases in fire emissions for central and eastern Europe that were due mainly to changes in population density, while climate change had a discernable impact only for RCP8.5 but not for RCP4.5.

Climate change in eastern Europe leads to warmer and drier growth conditions which affect vegetation structure and mortality rates, and therefore fuel type, fuel load, fire intensity, and rate of fire spread. Eastern (and southeastern) Europe is also a region where large-scale population decline is expected, particularly for SSP5 (Figure S5). The emerging trends in burned area were attributed to different drivers in LPJ-GUESS and LPJmL. As seen in Figure 7, climate and CO_2 affected burned area positively in both models. These effects were substantially stronger in LPJmL, arising from stronger climate-vegetation-fire interactions due to the higher sensitivity to changes in vegetation structure and fuel load.

In our study, eastern Europe emerged as an example region for the potentially important effects of changes in human population and population urban share. Both models assume that in sparsely populated areas, fires spread more easily, as fire detection takes longer, firefighting is delayed and fire spread is fostered in less-fragmented landscapes. High level of population density, in contrast, usually means less potential ignitions, considerable landscape fragmentation, and urbanization, all of which reduce fire spread [*Archibald et al.*, 2010; *Knorr et al.*, 2014]. SSP1 and SSP5 both assume declining population density (Figure S5c) and an increasing fraction of the population residing in urban environments (https://secure.iiasa.ac.at/web-apps/ene/SspDb/dsd?Action=htmlpage&page=countries) in the eastern parts of the continent over the 21st century. In LPJ-GUESS this translated into an overall increase in burned area with a strong contribution from human influence of similar magnitude to the climate effect, while the effect for LPJmL was negligible which echoed the small human effect found by *Migliavacca et al.* [2013b]. LPJ-GUESS characterizes fire based on an empirical model that integrates human effects on fire ignitions and fire spread. In line with *Guyette et al.* [2002], LPJ-GUESS assumes that an ignition-limited fire regime likely exists only under rare conditions of very low population density, and the suppression effect thus is dominant for most of Europe [*Knorr et al.*, 2014]. By contrast, LPJmL links fire density (number of fires per area and time interval) to population and assumes that the number of fires tends to increase with increasing population density up to about 16 people per square kilometer, declining thereafter [*Thonicke et al.*, 2010]. Consequently, for regions where projected changes in population density vary around this threshold, both increases and declines in burned area could occur, leading to a small net effect (Figure 5).

4.3. Mediterranean Europe: Will Changes in Fuel Load Matter?

By contrast to all other subregions, the simulated levels of increases in burned area over the 21st century for Mediterranean Europe were rather similar in both models (Figure 7, inset). However, similar to what was observed for eastern Europe, the underlying processes differed substantially. Both models found a strong

and positive CO_2 effect. However, in LPJ-GUESS, climate change was the slightly stronger driver which is in line with *Pechony and Shindell* [2010], who simulated positive fire activity trends driven by climate for this region. In LPJmL, climate change reduced fuel loads strongly, in turn constraining the overall trend of burned area and leading to a dominant negative climate effect. This strong interaction with vegetation agrees with *Pausas and Paula* [2012] and *Krawchuk et al.* [2009] who found that vegetation could play a strong role in wildfire distribution in Mediterranean Europe. For example, *Pausas and Paula* [2012] defined 13 regions for the Iberian Peninsula distributed along an aridity gradient with different vegetation productivity and fuel structure and found that the vegetation characteristics were statistically more relevant in driving fire activity than climatic conditions.

The different climate effects from the two models can be explained by the different underlying fire-vegetation interactions. SIMFIRE [*Knorr et al.*, 2014] applies FAPAR to represent fuel continuity, whereas SPITFIRE [*Thonicke et al.*, 2010] divides litter into dead fuel classes to account for the influence of fine and medium-size fuel on fire spread, thus burned area. By considering postfire mortality, trees can die after fire, and their dead biomass can contribute to litter accumulation during fire-free intervals leading to stronger fire impacts when a fire occurs in LPJmL eventually reducing woody vegetation. With vegetation growth increasingly limited, fuel load is reduced, thus limiting fire spread under climate change. This can impose a dominant negative effect on fire, despite increasing climatic fire danger. This explains why the vegetation-constraining effect for LPJmL is stronger, resulting in a negative climate effect on fire for Mediterranean Europe with obviously limited buffering effects of atmospheric CO_2 on vegetation growth, thus fire (Figure 7).

4.4. Northern Europe: Will Changes in Vegetation Composition Matter?

Northern Europe differs from the rest of Europe by its sparse population, and (even though most forests are managed) a comparatively natural response of vegetation species composition to climate change can be expected to be more visible than in other regions of the continent [*Peterken*, 1996]. In previous studies of past fire regimes for northern Europe, climate was identified as the main driver [e.g., *Pitkänen et al.*, 2002; *Carcaillet et al.*, 2007; *Olsson et al.*, 2010], but in addition to direct climate effects, interactions with species composition can also be important [*Pitkänen et al.*, 2002; *Tryterud*, 2003; *Brown and Giesecke*, 2014]. A historical example of this is the (re-)establishment of spruce in Scandinavia during the Holocene, which is thought to be initiated by climate, and which could then trigger a change from a (prespruce) fire-prone to a (postspruce) fire-free area [*Tryterud*, 2003; *Ohlson et al.*, 2011]. Observations such as these pose the question whether future climate change would also potentially lead to changes in natural vegetation types that could notably alter the future fire regime. Simulations with LPJ-GUESS indicated a future northward spread of conifer vegetation at the northern timberline, and broadleaf forest replacing mixed forest on the southern edge of their distribution [*Hickler et al.*, 2012] due to the combined effects of climate change and enhanced CO_2 concentration (also shown in Figure S4). These changes in vegetation type enlarged fire-free areas for parts of northern Europe (Figure 5a) because needleleaf forest is less prone to fire effects than the replaced high-latitude grassland, and broadleaf forest is less prone than mixed forest [*Knorr et al.*, 2014]. Similar large-scale vegetation shifts also operate in LPJmL. In addition, different fuel bulk densities parameterized for each PFTs and changing tree-to-grass ratios (Figure S4) influenced fire spread [*Thonicke et al.*, 2010], but the resulting fire-dampening effects did not outweigh climate change impacts at the large scale in northern Europe. Accordingly, climate change effects were the overall most dominant factors enhancing burned area in LPJmL as well.

4.5. Western Europe: A Region With Least Concern

Being densely populated, relatively wet, and dominated by agricultural lands, the present level of fire occurrence in western Europe is low, and very few studies have so far discussed possible changes in the fire regime of this region. Future burned area for western Europe was simulated to increase substantially by LPJmL but moderately by LPJ-GUESS, though the relative influence of the investigated drivers are comparable. The large intermodel difference in magnitude stems mainly from the climate effect and the CO_2 effect (Figure 7 "W. Europe" and Table S2) which are both closely associated with the uncertainty in fire-vegetation interactions (see also sections 4.3 and 4.4).

4.6. Model Comparison and Future Work

In our study, the two models simulated diverging, regionally heterogeneous changes in burned area. Large uncertainties exist not only due to diverging climate change and socioeconomic drivers but also due to

differing processes representation in the models. The semiempirical fire model SIMFIRE, incorporated in LPJ-GUESS represents fire as a simplified function of temperature, precipitation, population density, vegetation cover fraction expressed as FAPAR, and biome type. The number of degrees of freedom is thus expected to be smaller than SPITFIRE incorporated in LPJmL, which aims to provide highly detailed processes in simulating fire regime including fire spread, fire intensity, and postfire mortality of vegetation. But the intermodel differences shown in this study could be the result not only of the fire representation per se, but likely also arise from the simulated vegetation composition and structure. The explicit individual-based approach in LPJ-GUESS may have an advantage when representing vegetation dynamics in areas subject to pronounced seasonal water deficits [*Smith et al.*, 2001; *Hickler et al.*, 2012]. In the current presentation of SIMFIRE [*Knorr et al.*, 2014], fire-induced feedbacks to vegetation composition are limited, while fire effects in SPITFIRE [*Thonicke et al.*, 2010] affect average vegetation individuals of a specific PFT, thus likely overestimating the vegetation feedback.

For human-fire interactions, both models employ empirical methods based on different data sources or model assumptions. SIMFIRE parameterizes fire ignition and fire suppression based on remote sensing data using a semiempirical approach, leading to better model evaluation results compared to SPITFIRE. SPITFIRE quantifies human-caused fire ignitions based on a simple approximation of ignition scaling with human population density [*Venevsky et al.*, 2002], an approach that is now widely used in other global fire models [e.g., *Arora and Boer*, 2005; *Kloster et al.*, 2010] and confirmed to be applicable to Europe [*Migliavacca et al.*, 2013a]. However, by making the fire duration solely dependent on fire danger, SPITFIRE likely overestimates burned area in countries with sophisticated fire-fighting strategies. This could in part explain the overestimation of area burned in Mediterranean Europe under current climate found in this study. In other models fire ignitions and fire duration were calibrated for Europe at Nomenclature of Units for Territorial Statistics-3 level using fire-statistical data to improve simulation of burned area [*Migliavacca et al.*, 2013a]. This approach yields relatively low modeling error against remotely sensed and fire-statistical data, but it implies that the spatial distribution of fire ignitions and fire suppression remains constant over time, including climate change. The approaches presented in this study are based on dynamic representation of fire ignition and spread with different degree of vegetation-fire feedback mechanisms incorporated. Being more prone to error propagation, projected changes of future burned area are rather uncertain in Mediterranean Europe (LPJmL-SPITFIRE) and in northern Europe (LPJ-GUESS-SIMFIRE). However, they offer a first insight to possible future trajectories where the interactions between biotic and abiotic conditions, as well as human population density, may lead to nonlinear changes, e.g., new fire-prone areas or reduced burned area despite increased future climatic fire danger. It will be important to regionally refine process-based approaches for simulating human-caused ignitions and pattern of fire suppression (LPJmL-SPITFIRE) and improve feedback to vegetation composition and fuel limitation (LPJ-GUESS-SIMFIRE).

In addition, CO_2 fertilization effects on fuel availability and thus burned area could be altered by carbon-nitrogen (C-N) interactions under climate change. Results from a number of DGVMs indicate that N limitation limits the strength of CO_2 fertilization on terrestrial C sequestration, particularly so in boreal ecosystems. These interactions become less limiting toward temperate and tropical latitudes (see review article by *Zaehle and Dalmonech* [2011]). *Thornton et al.* [2007] have also argued that the CO_2 fertilization effect could be constrained by N limitation for the European continent. But coupled CN DGVM experiments also have shown that warmer climate will result in increasing soil mineralization rate and N availability to plants [*Zaehle and Dalmonech*, 2011; *Wårlind et al.*, 2014]. Therefore, as the large competing individual effects of N on carbon cycle processes cancel each other to some degree, a similar analysis will yet have to be performed regarding interactions of the coupled carbon and nitrogen cycle on fuel load, vegetation type, burned area, and fire emissions. Future land use and land cover could undergo considerable changes in Europe, at least in some regions, when global trade, technology, demography, and policies change [*Busch*, 2006]. Depending on the spatial pattern, this could lead to either decrease (due to reduction in naturally vegetated area) or increase (due to agriculture abandonment) in future burnt area as land use change alters fuel loads and fuel connectivity [*Power et al.*, 2010; *Viedma et al.*, 2015] but also use of fire on agricultural land. Due to large uncertainties involved with these aspects, we have included land use change only indirectly into our analysis by analyzing aspects of demography only. Clearly, once improved future projections of land use and land cover change scenarios at the continental scale become available, these could be also considered for European future fire regimes.

5. Summary

In this study, we used climate projections from four ESMs for two radiative concentration pathways (RCP8.5 and RCP2.6) and two socioeconomic scenarios to investigate future impacts on fire. We specifically analyzed the relative contribution of climate change, atmospheric CO_2, and human population on future burned area for Europe from two fire-vegetation models.

We found that climate change is not necessarily the dominant driver for future fire regime for Europe (highest RFE in individual model: 64% of RFE_{CC} in LPJ-GUESS versus 223% of RFE_{CO2} in LPJmL) when considering interactions with vegetation, as seen by the large response of fire to CO_2 fertilization. The influence of vegetation is important and outweighed the effect of population density for most parts of Europe. Eastern Europe, with a substantial increase in future burned area simulated by both models, could be a potential new fire-prone area in future and should gain attention in future fire management. Changes in future burned area for Mediterranean and northern Europe are less robust due to the uncertainty in fire-vegetation interaction.

Acknowledgments

This work was supported by EU contracts 243888 (forest fires under climate, social and economic changes in Europe, the Mediterranean, and other fire-affected areas of the world, FUME) and 265148 (pan-European gas and aerosols study, PEGASOS). A.A. also acknowledges support by EU grant FP 7 LUC4C (grant 603542) and the Formas Strong REsearch Environment Landuse today and tomorrow (LUsTT). We acknowledge the World Climate Research Programme's Working Group on Coupled Modelling, which is responsible for CMIP, and we thank the climate modeling groups (listed in Table 1 of this paper) for producing and making available their model output. For CMIP the US Department of Energy's Program for Climate Model Diagnosis and Intercomparison provides coordinating support and led development of software infrastructure in partnership with the Global Organization for Earth System Science Portals. We thank JRC for making the EFFIS data available. EFFIS data were provided by the European Forest Fire Information System-EFFIS (http://effis.jrc.ec.europa.eu) of the European Commission Joint Research Centre. M.C.W. would like to thank Anders Ahlström, Niklas Olén, and Jan Hendrik Blanke for their kind supports and helpful discussion.

References

Ahlström, A., G. Schurgers, A. Arneth, and B. Smith (2012), Robustness and uncertainty in terrestrial ecosystem carbon response to CMIP5 climate change projections, *Environ. Res. Lett.*, *7*(4), 044008.

Amatulli, G., A. Camia, and J. San-Miguel-Ayanz (2013), Estimating future burned areas under changing climate in the EU-Mediterranean countries, *Sci. Total Environ.*, *450*, 209–222.

Archibald, S., R. J. Scholes, D. P. Roy, G. Roberts, and L. Boschetti (2010), Southern African fire regimes as revealed by remote sensing, *Int. J. Wildland Fire*, *19*(7), 861–878, doi:10.1071/WF10008.

Arora, V. K., and G. J. Boer (2005), Fire as an interactive component of dynamic vegetation models, *J. Geophys. Res.*, *110*, G02008, doi:10.1029/2005JG000042.

Bond, W., F. Woodward, and G. Midgley (2005), The global distribution of ecosystems in a world without fire, *New Phytol.*, *165*(2), 525–538.

Bondeau, A., P. C. Smith, S. Zaehle, S. Schaphoff, W. Lucht, W. Cramer, D. Gerten, H. Lotze-Campen, C. Müller, and M. Reichstein (2007), Modelling the role of agriculture for the 20th century global terrestrial carbon balance, *Global Change Biol.*, *13*(3), 679–706.

Bowman, D. M. J. S., and W. J. Panton (1995), Munmarlary revisited: Response of a north Australian Eucalyptus tetrodonta savanna protected from fire for 20 years, *Aust. J. Ecol.*, *20*(4), 526–531.

Bowman, D. M. J. S., J. K. Balch, P. Artaxo, W. J. Bond, J. M. Carlson, M. A. Cochrane, C. M. D'Antonio, R. S. DeFries, J. C. Doyle, and S. P. Harrison (2009), Fire in the Earth system, *Science*, *324*(5926), 481–484.

Brown, K. J., and T. Giesecke (2014), Holocene fire disturbance in the boreal forest of central Sweden, *Boreas*, *43*(3), 639–651.

Busch, G. (2006), Future European agricultural landscapes—What can we learn from existing quantitative land use scenario studies?, *Agric., Ecosyst. Environ.*, *114*(1), 121–140.

Camia, A., T. D. Houston, and J. San-Miguel-Ayanz (2010), The European fire database: Development, structure and implementation, *6th Intl. Conf. on For. Fire Res. A20*, Coimbra, Portugal.

Carcaillet, C., I. Bergman, S. Delorme, G. Hornberg, and O. Zackrisson (2007), Long-term fire frequency not linked to prehistoric occupations in northern Swedish boreal forest, *Ecology*, *88*(2), 465–477.

Ciais, P., et al. (2013), Carbon and other biogeochemical cycles, in *Climate Change 2013: The Physical Science Basis. Contribution of Working Group I to the Fifth Assessment Report of the Intergovernmental Panel on Climate Change*, edited by T. F. Stocker et al., pp. 465–570, Cambridge Univ. Press, Cambridge, U. K., and New York, doi:10.1017/CBO9781107415324.015.

Cramer, W., A. Bondeau, F. I. Woodward, I. C. Prentice, R. A. Betts, V. Brovkin, P. M. Cox, V. Fisher, J. A. Foley, and A. D. Friend (2001), Global response of terrestrial ecosystem structure and function to CO_2 and climate change: Results from six dynamic global vegetation models, *Global Change Biol.*, *7*(4), 357–373.

Daniau, A. L., S. P. Harrison, and P. J. Bartlein (2010), Fire regimes during the Last Glacial, *Quat. Sci. Rev.*, *29*(21–22), 2918–2930, doi:10.1016/j.quascirev.2009.11.008.

Fader, M., D. Gerten, M. Thammer, J. Heinke, H. Lotze-Campen, W. Lucht, and W. Cramer (2011), Internal and external green-blue agricultural water footprints of nations, and related water and land savings through trade, *Hydrol. Earth Syst. Sci.*, *15*(5), 1641–1660, doi:10.5194/hess-15-1641-2011.

Flannigan, M. D., B. J. Stocks, and B. M. Wotton (2000), Climate change and forest fires, *Sci. Total Environ.*, *262*(3), 221–229, doi:10.1016/S0048-9697(00)00524-6.

Flannigan, M. D., K. Logan, B. Amiro, W. Skinner, and B. Stocks (2005), Future area burned in Canada, *Clim. Change*, *72*(1–2), 1–16.

Ganteaume, A., A. Camia, M. Jappiot, J. San-Miguel-Ayanz, M. Long-Fournel, and C. Lampin (2013), A review of the main driving factors of forest fire ignition over Europe, *Environ. Manage.*, *51*(3), 651–662.

Giglio, L., J. T. Randerson, G. R. Werf, P. S. Kasibhatla, G. J. Collatz, D. C. Morton, and R. S. DeFries (2010), Assessing variability and long-term trends in burned area by merging multiple satellite fire products, *Biogeosciences*, *7*(3), 1171–1186.

Goldewijk, K. K., A. Beusen, and P. Janssen (2010), Long-term dynamic modeling of global population and built-up area in a spatially explicit way: HYDE 3.1, *Holocene*, *20*(4), 565–573.

Guyette, R. P., R. Muzika, and D. C. Dey (2002), Dynamics of an anthropogenic fire regime, *Ecosystems*, *5*(5), 472–486.

Harris, I., P. Jones, T. Osborn, and D. Lister (2014), Updated high-resolution grids of monthly climatic observations–the CRU TS3. 10 Dataset, *Int. J. Climatol.*, *34*(3), 623–642.

Hickler, T., B. Smith, I. C. Prentice, K. Mjöfors, P. Miller, A. Arneth, and M. T. Sykes (2008), CO_2 fertilization in temperate FACE experiments not representative of boreal and tropical forests, *Global Change Biol.*, *14*(7), 1531–1542.

Hickler, T., K. Vohland, J. Feehan, P. A. Miller, B. Smith, L. Costa, T. Giesecke, S. Fronzek, T. R. Carter, and W. Cramer (2012), Projecting the future distribution of European potential natural vegetation zones with a generalized, tree species-based dynamic vegetation model, *Global Ecol. Biogeogr.*, *21*(1), 50–63.

Hollander, M., and D. A. Wolfe (1999), *Nonparametric Statistical Methods*, pp. 35–140, John Wiley, New York.

Jiang, L. (2014), Internal consistency of demographic assumptions in the shared socioeconomic pathways, *Popul. Environ.*, *35*(3), 261–285, doi:10.1007/s11111-014-0206-3.
Johnson, E. A. (1992), *Fire and Vegetation Dynamics: Studies From the North American Boreal Forest*, pp. 129, Cambridge Univ. Press, Cambridge, U. K.
Kloster, S., N. M. Mahowald, J. T. Randerson, P. E. Thornton, F. M. Hoffman, S. Levis, P. J. Lawrence, J. J. Feddema, K. W. Oleson, and D. M. Lawrence (2010), Fire dynamics during the 20th century simulated by the Community Land Model, *Biogeosci. Discuss.*, *7*(1), 565–630.
Kloster, S., N. Mahowald, J. Randerson, and P. Lawrence (2012), The impacts of climate, land use, and demography on fires during the 21st century simulated by CLM-CN, *Biogeosciences*, *9*, 509–525.
Knorr, W., V. Lehsten, and A. Arneth (2012), Determinants and predictability of global wildfire emissions, *Atmos. Chem. Phys.*, *12*(15), 6845–6861.
Knorr, W., T. Kaminski, A. Arneth, and U. Weber (2014), Impact of human population density on fire frequency at the global scale, *Biogeosciences*, *11*(4), 1085–1102.
Knorr, W., L. Jiang, and A. Arneth (2015), Climate, CO_2, and demographic impacts on global wildfire emissions, *Biogeosci. Discuss.*, *12*(17), 15,011–15,050, doi:10.5194/bgd-12-15011-2015.
Krawchuk, M. A., M. A. Moritz, M.-A. Parisien, J. Van Dorn, and K. Hayhoe (2009), Global pyrogeography: The current and future distribution of wildfire, *PLoS One*, *4*(4), e5102, doi:10.1371/journal.pone.0005102.
Marlon, J. R., P. J. Bartlein, C. Carcaillet, D. G. Gavin, S. P. Harrison, P. E. Higuera, F. Joos, M. J. Power, and I. C. Prentice (2008), Climate and human influences on global biomass burning over the past two millennia, *Nat. Geosci.*, *1*(10), 697–702, doi:10.1038/ngeo313.
McCarty, J. L., S. Korontzi, C. O. Justice, and T. Loboda (2009), The spatial and temporal distribution of crop residue burning in the contiguous United States, *Sci. Total Environ.*, *407*(21), 5701–5712.
McWethy, D. B., C. Whitlock, J. M. Wilmshurst, M. S. McGlone, M. Fromont, X. Li, A. Dieffenbacher-Krall, W. O. Hobbs, S. C. Fritz, and E. R. Cook (2010), Rapid landscape transformation in South Island, New Zealand, following initial Polynesian settlement, *Proc. Natl. Acad. Sci. U.S.A.*, *107*(50), 21,343–21,348.
Migliavacca, M., A. Dosio, S. Kloster, D. Ward, A. Camia, R. Houborg, T. Houston Durrant, N. Khabarov, A. Krasovskii, and S. Miguel-Ayanz (2013a), Modeling burned area in Europe with the Community Land Model, *J. Geophys. Res. Biogeosci.*, *118*, 265–279, doi:10.1002/jgrg.20026.
Migliavacca, M., et al. (2013b), Modeling biomass burning and related carbon emissions during the 21st century in Europe, *J. Geophys. Res. Biogeosci.*, *118*, 1732–1747, doi:10.1002/2013JG002444.
Moreira, A. G. (2000), Effects of fire protection on savanna structure in Central Brazil, *J. Biogeogr.*, *27*(4), 1021–1029.
Moreira, F., et al. (2011), Landscape – wildfire interactions in southern Europe: Implications for landscape management, *J. Environ. Manage.*, *92*(10), 2389–2402, doi:10.1016/j.jenvman.2011.06.028.
Moreno, J. M., A. Vázquez, and R. Vélez (1998), Recent history of forest fires in Spain, in *Large Forest Fires*, edited by J. M. Moreno, pp. 159–185, Backhuys, Leiden, Netherlands.
Moriondo, M., P. Good, R. Durao, M. Bindi, C. Giannakopoulos, and J. Corte-Real (2006), Potential impact of climate change on fire risk in the Mediterranean area, *Clim. Res.*, *31*(1), 85–95.
Mouillot, F., and C. B. Field (2005), Fire history and the global carbon budget: A 1×1 fire history reconstruction for the 20th century, *Global Change Biol.*, *11*(3), 398–420.
Mouillot, F., S. Rambal, and R. Joffre (2002), Simulating climate change impacts on fire frequency and vegetation dynamics in a Mediterranean-type ecosystem, *Global Change Biol.*, *8*(5), 423–437.
Ohlson, M., K. J. Brown, H. J. B. Birks, J. A. Grytnes, G. Hörnberg, M. Niklasson, H. Seppä, and R. H. Bradshaw (2011), Invasion of Norway spruce diversifies the fire regime in boreal European forests, *J. Ecol.*, *99*(2), 395–403.
Olsson, F., M.-J. Gaillard, G. Lemdahl, A. Greisman, P. Lanos, D. Marguerie, N. Marcoux, P. Skoglund, and J. Wäglind (2010), A continuous record of fire covering the last 10,500 calendar years from southern Sweden—The role of climate and human activities, *Palaeogeogr. Palaeoclimatol. Palaeoecol.*, *291*(1), 128–141.
O'Neill, B. C., E. Kriegler, K. Riahi, K. L. Ebi, S. Hallegatte, T. R. Carter, R. Mathur, and D. P. van Vuuren (2014), A new scenario framework for climate change research: The concept of shared socioeconomic pathways, *Clim. Change*, *122*(3), 387–400.
Pausas, J. G., and S. Paula (2012), Fuel shapes the fire–climate relationship: Evidence from Mediterranean ecosystems, *Global Ecol. Biogeogr.*, *21*(11), 1074–1082.
Pechony, O., and D. Shindell (2010), Driving forces of global wildfires over the past millennium and the forthcoming century, *Proc. Natl. Acad. Sci. U.S.A.*, *107*(45), 19,167–19,170.
Peterken, G. F. (1996), *Natural Woodland: Ecology and Conservation in Northern Temperate Regions*, Cambridge Univ. Press, Cambridge.
Pitkänen, A., P. Huttunen, H. Jungner, and K. Tolonen (2002), A 10 000 year local forest fire history in a dry heath forest site in eastern Finland, reconstructed from charcoal layer records of a small mire, *Can. J. For. Res.*, *32*(10), 1875–1880.
Power, M. J., J. R. Marlon, P. J. Bartlein, and S. P. Harrison (2010), Fire history and the Global Charcoal Database: A new tool for hypothesis testing and data exploration, *Palaeogeogr. Palaeoclimatol. Palaeoecol.*, *291*(1–2), 52–59, doi:10.1016/j.palaeo.2009.09.014.
Ramankutty, N., and J. A. Foley (1999), Estimating historical changes in global land cover: Croplands from 1700 to 1992, *Global Biogeochem. Cycles*, *13*(4), 997–1027, doi:10.1029/1999GB900046.
Randerson, J., H. Liu, M. Flanner, S. Chambers, Y. Jin, P. Hess, G. Pfister, M. Mack, K. Treseder, and L. Welp (2006), The impact of boreal forest fire on climate warming, *Science*, *314*(5802), 1130–1132.
Randerson, J., Y. Chen, G. Werf, B. Rogers, and D. Morton (2012), Global burned area and biomass burning emissions from small fires, *J. Geophys. Res.*, *117*, G04012, doi:10.1029/2012JG002128.
Roebroeks, W., and P. Villa (2011), On the earliest evidence for habitual use of fire in Europe, *Proc. Natl. Acad. Sci. U.S.A.*, *108*(13), 5209–5214.
San-Miguel-Ayanz, J., J. M. Moreno, and A. Camia (2013), Analysis of large fires in European Mediterranean landscapes: Lessons learned and perspectives, *For. Ecol. Manage.*, *294*, 11–22.
Savage, M., and T. W. Swetnam (1990), Early 19th-century fire decline following sheep pasturing in a Navajo ponderosa pine forest, *Ecology*, *71*(6), 2374–2378.
Schmuck, G., J. San-Miguel-Ayanz, A. Camia, T. Durrant, S. Santos de Oliveira, R. Boca, C. Whitmore, C. Giovando, G. Libertá, and P. Corti (2011), Forest fires in Europe 2010, *Joint Research Centre–Institute for Environment and Sustainability Eur*, *24910*.
Schmuck, G., J. San-Miguel-Ayanz, A. Camia, T. H. Durrant, R. Boca, G. Libertá, T. Petroliagkis, M. Di Leo, D. Rodriguez-Aseretto, and F. Boccacci (2014), Forest fires in Europe, Middle East and North Africa 2013, vol. 26791, doi:10.2788/99870.
Shackleton, C., and R. Scholes (2000), Impact of fire frequency on woody community structure and soil nutrients in the Kruger National Park, *Koedoe-African Prot. Area Conserv. Sci.*, *43*(1), 75–81.

Sitch, S., et al. (2003), Evaluation of ecosystem dynamics, plant geography and terrestrial carbon cycling in the LPJ dynamic global vegetation model, *Global Change Biol.*, *9*(2), 161–185.

Smith, B., I. C. Prentice, and M. T. Sykes (2001), Representation of vegetation dynamics in the modelling of terrestrial ecosystems: Comparing two contrasting approaches within European climate space, *Global Ecol. Biogeogr.*, *10*(6), 621–637, doi:10.1046/j.1466-822X.2001.t01-1-00256.x.

Sun, Y., L. Gu, R. E. Dickinson, R. J. Norby, S. G. Pallardy, and F. M. Hoffman (2014), Impact of mesophyll diffusion on estimated global land CO2 fertilization, *Proc. Natl. Acad. Sci. U.S.A.*, *111*(44), 15,774–15,779, doi:10.1073/pnas.1418075111.

Taylor, K. E., R. J. Stouffer, and G. A. Meehl (2012), An overview of CMIP5 and the experiment design, *Bull. Am. Meteorol. Soc.*, *93*(4), 485–498.

Thonicke, K., and W. Cramer (2006), Long-term trends in vegetation dynamics and forest fires in Brandenburg (Germany) under a changing climate, *Nat. Hazards*, *38*(1–2), 283–300.

Thonicke, K., A. Spessa, I. C. Prentice, S. P. Harrison, L. Dong, and C. Carmona-Moreno (2010), The influence of vegetation, fire spread and fire behaviour on biomass burning and trace gas emissions: Results from a process-based model, *Biogeosciences*, *7*(6), 1991–2011.

Thornton, P. E., J. F. Lamarque, N. A. Rosenbloom, and N. M. Mahowald (2007), Influence of carbon-nitrogen cycle coupling on land model response to CO_2 fertilization and climate variability, *Global Biogeochem. Cycles*, *21*, GB4018, doi:10.1029/2006GB002868.

Tryterud, E. (2003), Forest fire history in Norway: From fire-disturbed pine forests to fire-free spruce forests, *Ecography*, *26*(2), 161–170, doi:10.1034/j.1600-0587.2003.02942.x.

van der Werf, G. R., J. T. Randerson, L. Giglio, N. Gobron, and A. Dolman (2008), Climate controls on the variability of fires in the tropics and subtropics, *Global Biogeochem. Cycles*, *22*, GB3028, doi:10.1029/2007GB003122.

van Vuuren, D., and T. R. Carter (2014), Climate and socio-economic scenarios for climate change research and assessment: Reconciling the new with the old, *Clim. Change*, *122*(3), 415–429.

van Vuuren, D., et al. (2011), The representative concentration pathways: An overview, *Clim. Change*, *109*(1–2), 5–31, doi:10.1007/s10584-011-0148-z.

Venevsky, S., K. Thonicke, S. Sitch, and W. Cramer (2002), Simulating fire regimes in human-dominated ecosystems: Iberian Peninsula case study, *Global Change Biol.*, *8*(10), 984–998.

Viedma, O., N. Moity, and J. M. Moreno (2015), Changes in landscape fire-hazard during the second half of the 20th century: Agriculture abandonment and the changing role of driving factors, *Agric., Ecosyst. Environ.*, *207*, 126–140, doi:10.1016/j.agee.2015.04.011.

Wårlind, D., B. Smith, T. Hickler, and A. Arneth (2014), Nitrogen feedbacks increase future terrestrial ecosystem carbon uptake in an individual-based dynamic vegetation model, *Biogeosciences*, *11*(21), 6131–6146, doi:10.5194/bg-11-6131-2014.

Westerling, A. L., H. G. Hidalgo, D. R. Cayan, and T. W. Swetnam (2006), Warming and earlier spring increase western US forest wildfire activity, *Science*, *313*(5789), 940–943.

Zaehle, S., and D. Dalmonech (2011), Carbon–nitrogen interactions on land at global scales: Current understanding in modelling climate biosphere feedbacks, *Curr. Opin. Environ. Sustainability*, *3*(5), 311–320.